

Analysis of Neutron Stars Observations Using a Correlated Fermi Gas Model

O. Hen,¹ A.W. Steiner,^{2,3,4} E. Piasezky,⁵ and L.B. Weinstein⁶

¹*Massachusetts Institute of Technology, Cambridge, MA 02139, USA*

²*Institute for Nuclear Theory, University of Washington, Seattle, Washington 98195, USA*

³*Department of Physics and Astronomy, University of Tennessee, Knoxville, Tennessee 37996, USA*

⁴*Physics Division, Oak Ridge National Laboratory, Oak Ridge, Tennessee 37831, USA*

⁵*Tel Aviv University, Tel Aviv 69978, Israel*

⁶*Old Dominion University, Norfolk, VA 23529, USA*

(Dated: August 2, 2016)

Background: The nuclear symmetry energy is a fundamental ingredient in determining the equation of state (EOS) of neutron stars (NS). Recent terrestrial experiments constrain both its value and slope at nuclear saturation density, however, its value at higher densities is unknown. Assuming a Free Fermi-gas (FFG) model for the kinetic symmetry energy, the high-density extrapolation depends on a single parameter, the density dependence of the potential symmetry energy. The Correlated Fermi-gas (CFG) model improves on the FFG model by including the effects of short-range, correlated, high-momentum, nucleons in nuclear matter. Using the CFG model for the kinetic symmetry energy along with constraints from terrestrial measurements leads to a much softer density dependence for the potential symmetry energy.

Purpose: Examine the ability of the FFG and CFG models to describe NS observables that are directly sensitive to the symmetry energy at high-density. Specifically, examine the ability of the CFG model, with its softer density dependence of the potential symmetry energy, to describe a two solar-mass NS.

Methods: Using a Bayesian analysis of NS observables, we use the CFG and FFG models to describe the symmetry energy and examine the resulting parameters in the NS EOS and the density dependence of the potential symmetry energy.

Results: Despite the large difference in the density dependence of the potential part of the symmetry energy, both models can describe the NS data and support a two solar-mass NS. The different density dependences has only a small effect on the NS EOS.

Conclusions: While sensitive to the high-density values of the symmetry energy, NS observables alone are not enough to distinguish between the CFG and FFG models. This indicates that the NS EOS, obtain from Bayesian analysis of NS observables, is robust and is not sensitive to the exact nuclear model used for the kinetic part of the nuclear symmetry energy.

PACS numbers:

INTRODUCTION

Determining the equation of state (EOS) of dense nuclear matter, such as that found in neutron stars (NS), is a long-sought goal of nuclear physics. The EOS is a fundamental property of quantum chromodynamics and is an observable independent of renormalization scale and scheme. While considerable progress had been made in theoretical studies of nuclear and neutron matter at high densities [1–3], experimental constraints from terrestrial experiments and astrophysical observations are still sparse.

One of the largest uncertainties in the NS EOS is the density dependence of the nuclear symmetry energy [4]. This describes the change in the energy of nuclear matter as one replaces a proton with a neutron. The symmetry energy is constrained by terrestrial measurements up to nuclear saturation density, ρ_0 ($= 0.16$ nucleons/fm³ ≈ 160 MeV/fm³) [5–12]. Specifically at saturation density, the value and slope of the symmetry energy were recently determined to within an accuracy of about ± 3 MeV and ± 20 MeV respectively [5, 6]. The symmetry

energy behavior at supra-nuclear densities, required for the description of NS, is not well known.

A common method used to simplify the extraction of the density dependence of the symmetry energy is to split the symmetry energy into kinetic and potential parts and study them separately [13]. The kinetic term is usually determined analytically using a zero-temperature Free-Fermi Gas (FFG) model, which fully determines the value at saturation density and the density dependence to supra-nuclear densities. Combined with the known total symmetry energy at saturation density, this determines the potential symmetry energy at saturation density, leaving its density dependence as the only unknown [13, 14].

While the analytical FFG model is simple and easy to use, it fails to describe many relevant properties of nuclear systems. In particular, microscopic calculations have shown that the FFG model underestimates the kinetic energy carried by nucleons in nuclei and nuclear matter [1, 15–19]. In addition, the FFG parameterization fails to accurately describe quantum Monte Carlo calculations of pure neutron matter [2]. Results from recent electron-scattering experiments indicate that 20

to 25% of nucleons in medium and heavy nuclei have momentum greater than the Fermi momentum [20–22]. These high-momentum nucleons dominate the kinetic energy of nucleons in nuclei and are predominantly in the form of neutron-proton (np) short-range correlated (SRC) pairs [23–28]. These SRC pairs are pairs of nucleons with large relative momentum and small center-of-mass momentum, where large and small are relative to the Fermi momentum. By neglecting these SRC pairs, the FFG model significantly underestimates the kinetic energy carried by nucleons in nuclei [29].

The effect of np-SRC pairs on the nuclear symmetry energy was recently investigated using the Correlated Fermi-Gas (CFG) model [29]. This model describes the momentum distribution of nucleons in symmetric nuclear-matter by:

$$n_{SNM}^{SRC}(k) = \begin{cases} A_0 & k < k_F \\ C_\infty/k^4 & k_F < k < \lambda k_F^0 \\ 0 & k > \lambda k_F^0 \end{cases} \quad (1)$$

where A_0 describes a depleted Fermi gas distribution that extends up to k_F , the density dependent Fermi momentum. Above the Fermi momentum the momentum distribution is dominated by np-SRC pairs and falls off as C_∞/k^4 [30]. This high momentum tail extends from k_F to a constant cutoff given by λk_F^0 , where k_F^0 is the Fermi-momentum of symmetric nuclear matter at saturation density. All constants in Eq. 1 (e.g., $C_\infty = c_0 k_F$ where $c_0 = 4.16 \pm 0.95$ and $\lambda = 2.75 \pm 0.25$) are extracted from data, see Ref. [29] for details.

The kinetic symmetry energy calculated using the FFG and the CFG models differ significantly. At saturation density, the FFG kinetic symmetry energy is either 12.5 or 17.0 MeV and the CFG kinetic symmetry energy ranges from -2.5 to -17.5 MeV [29]. The density dependences of the kinetic symmetry energy also differ. The FFG kinetic symmetry energy is proportional to $\rho^{2/3}$ while the CFG kinetic symmetry has terms proportional to $\rho^{1/3}$, $\rho^{2/3}$, and ρ .

The total symmetry energy equals the sum of the kinetic and potential symmetry energies. Since the value ($29 \text{ MeV} < E_{sym}(\rho_0) < 36 \text{ MeV}$) and density dependence ($30 \text{ MeV} < L = 3\rho \frac{\partial E_{sym}(\rho)}{\partial \rho} |_{\rho_0} < 70 \text{ MeV}$) of the total symmetry energy are known at saturation density [5], the value and density dependence of the potential symmetry energy will depend on the model used for the kinetic symmetry energy.

This work examines the sensitivity of the NS EOS, extracted from Bayesian analysis of NS mass and radius observations [14], to the inclusion of np-SRC using the CFG model. This is a complementary and independent approach to the previous use of terrestrial observations at saturation density and has a larger sensitivity to the high-density behavior of the symmetry energy.

We start with a short overview of NS observables, EOS parameterizations, and Bayesian analysis used to con-

strain free parameters in the NS EOS. We then discuss our results with emphasis on similarities and differences in the NS EOS obtained using the FFG and CFG models. We highlight the robustness of the resulting EOS and discuss the differences in the extracted potential symmetry energy.

BAYESIAN ANALYSIS OF NS OBSERVABLES AND THE NS EOS

Bayesian analysis allows constraining the NS EOS by performing a global fit of NS EOS to NS mass-radius extractions, taking into account external constraints from terrestrial measurements, astrophysical observations (e.g., observation of a two solar-mass NS) and physical limitations such as causality (i.e., speed of sound \leq speed of light), and hydrodynamical stability [14, 31].

The NS observations used in the analysis presented here include high precision mass extractions from Pulsar-timing measurements, simultaneous mass-radius extractions from photospheric radius expansion (PRE) X-ray burst measurements, and thermal spectra measurement of low-mass X-ray Binaries (LMXB), see Ref. [31] for details.

The parameterization of the NS EOS is divided into three energy-density regions: low ($\leq 15 \text{ MeV}/\text{fm}^3$), medium (15 to $\approx 350 \text{ MeV}/\text{fm}^3$), and high ($\leq \approx 350 \text{ MeV}/\text{fm}^3$). The low energy-density region describes the NS crust and its functional form is assumed to be

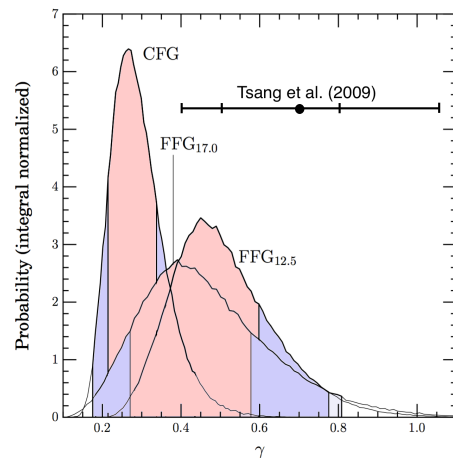


FIG. 1: (color online) The probability distribution of the extracted potential symmetry energy density dependence parameter γ (detailed in Eq. 3), obtained from a Bayesian analysis of NS observations using the CFG, FFG_{12.5}, and FFG_{17.0} models for the kinetic symmetry energy. The inner and outer shaded region mark the 1- and 2- σ limits of each distribution, see text for details. The horizontal line shows the centroid and one- and two-sigma limits from an analysis of heavy-ion collision data [13].

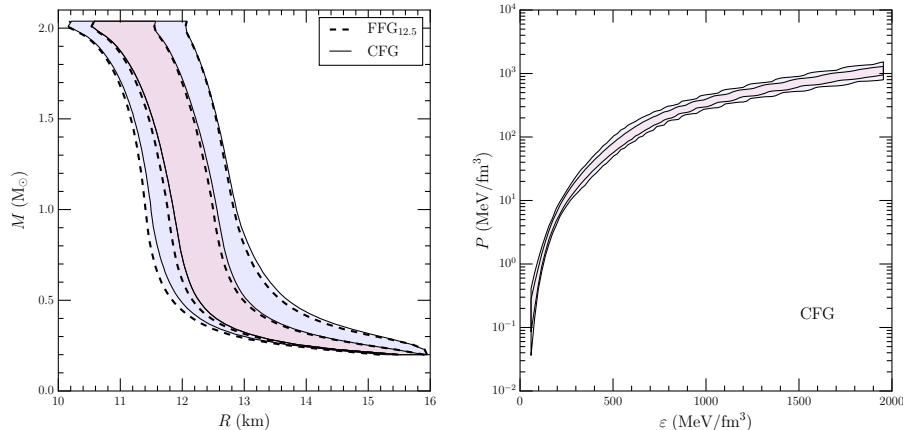


FIG. 2: The extracted mass-radius (left) and pressure energy-density (right) relations for the CFG (solid line) and FFG_{12.5} (dashed line) models. The results for the FFG_{12.5} and FFG₁₇ models are almost identical. The inner and outer contours show the one- and two-sigma results.

well constrained. The high energy-density region is parameterized by a one or two polytropes. The medium energy-density region has a physically motivated functional form, with two fit parameters (Incompressibility, K , and Skewness, κ) and the density dependent symmetry energy. See Ref. [14] for details.

As described in the introduction, the total symmetry energy is generally given by:

$$E_{sym}(\rho/\rho_0) = E_{sym}^{kin}(\rho/\rho_0) + E_{sym}^{pot}(\rho/\rho_0), \quad (2)$$

where $E_{sym}^{kin}(\rho/\rho_0)$ and $E_{sym}^{pot}(\rho/\rho_0)$ are the kinetic and potential parts of the total symmetry energy. At nuclear saturation density the total symmetry energy, S_v , and its slope, L , are well constrained by terrestrial measurements [5, 6]. The kinetic term can be analytically calculated assuming a FFG or CFG model, and the potential symmetry energy at saturation energy is calculated as: $S_{pot} = S_v - S_{kin}$, where S_{kin} is the kinetic symmetry energy at saturation density. The density dependence of the potential symmetry energy is parameterized as:

$$\begin{aligned} E_{sym}^{pot}(\rho/\rho_0) &= S_{pot} \cdot (\rho/\rho_0)^\gamma \\ &= (S_v - S_{kin}) \cdot (\rho/\rho_0)^\gamma, \end{aligned} \quad (3)$$

where, assuming knowledge of S_{kin} , γ is the only unknown.

To constrain the NS EOS in a self-consistent way, we follow Steiner et al. [14] and perform a Bayesian analysis of all available NS observations and terrestrial constraints on S and L , using the FFG or the CFG models to express the kinetic symmetry energy at saturation and its density dependence. Previous studies used the FFG model with either a free nucleon or an effective nucleon mass, resulting in $S_{kin} = 12.5$ and 17.0 MeV respectively [13, 14]. We examine both options and refer to them as FFG_{12.5} and FFG_{17.0} respectively.

BAYESIAN ANALYSIS RESULTS

We start by examining the details of the potential symmetry energy. Fig. 1 shows the density dependence of the potential symmetry energy for the three models. As can be seen, this variable is very sensitive to the choice of the kinetic symmetry energy model. The CFG kinetic symmetry energy is significantly lower than that of the FFG at saturation density. Because the total symmetry energy and its slope are fixed at saturation density, this increases the potential symmetry energy at ρ_0 and drastically decreases its density dependence, γ .

We note that the results shown in Fig. 1 for the FFG_{17.0} model differ from the ones previously obtained from a similar Bayesian analysis using the FFG_{17.0} model [14]. This difference is due to the inclusion of additional observations in the analysis described here and the expansion of the allowed range for γ down to zero to allow a clear comparison with the CFG model. Unlike previous works, the density dependence (γ) obtained using the FFG models are consistent with that extracted from heavy-ion analysis using the FFG_{12.5} model [13].

The dramatically different potential symmetry energy and density dependence obtained using the CFG and FFG models does not appear to have a large effect on the bulk properties of the resulting NS EOS. Fig. 2 shows the EOS obtained from the Bayesian analysis using the CFG and FFG_{12.5} models (the FFG_{12.5} and FFG_{17.0} models give almost identical results). Notice that despite the soft density dependence of the potential symmetry energy, the CFG EOS supports a two solar-mass NS.

Fig. 3 shows the extracted energy per nucleon as a function of the baryonic density for the CFG and FFG_{12.5} models (results for the FFG_{17.0} model are practically identical to the FFG_{12.5} model). The FFG results here are also very similar to the CFG model, although the

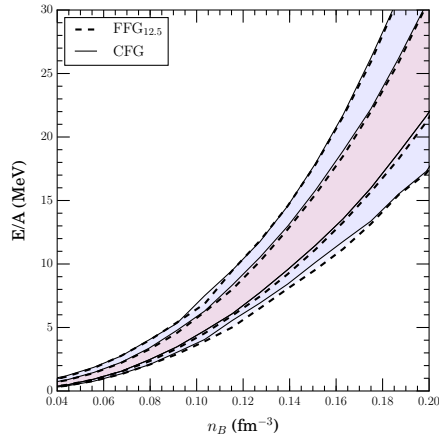


FIG. 3: (color online) The extracted energy per particle as a function of the baryonic density for the CFG (solid lines) and FFG_{12.5} (dashed lines) models. The results of the FFG_{12.5} and FFG₁₇ models are almost identical. The inner and outer contours show the one- and two-sigma limits. Both models are consistent with the empirical value of 16 MeV at saturation density.

latter yields a slightly larger energy. Both models are consistent with the empirical value of $E/A = 16$ MeV at saturation density.

The almost identical EOS and energy-density relations for the CFG, FFG_{12.5} and FFG_{17.0} models (as shown in Figs. 2 and 3) support the robustness of the Bayesian analysis and indicates that it is insensitive to the exact nuclear model used for the kinetic term of the nuclear symmetry energy. This is not surprising, since these are bulk properties of nuclear matter, which depend on the sum of the kinetic and potential symmetry energies (which is the same for both the CFG and FFG models).

The bulk properties of NS are robust and largely insensitive to the choice of the kinetic symmetry energy model. However, it is desired to know (1) which model captures the nuclear dynamics better and (2) whether there are other observables that can differentiate between them? Recent calculations done using a Relativistic Mean-Field (RMF) model for the symmetry potential obtained very different results for the nuclear incompressibility when calculated using the CFG and FFG models [32]. The result of the CFG model was consistent with recent experimental constraints. Another possible test could come from pion production and isospin diffusion observables measured in intermedium-energy heavy-ion collisions. These observables are directly sensitive to the potential symmetry energy but are traditionally analyzed using transport models that only incorporate the FFG model. By incorporating SRCs into transport models one could possibly differentiate between the FFG and CFG models.

SUMMARY

The kinetic part of the nuclear symmetry energy can be parametrized using two models: CFG and FFG. The CFG model includes short-range high-momentum pairs of nucleons in nuclei; the FFG model does not. Using Bayesian analysis of NS observables, we examined the ability of the CFG and FFG models to describe the data and examined the resulting parameters in the NS EOS and the density dependence of the potential symmetry energy. We find that both models can describe the data and support a two solar-mass NS. The obtained density dependence for the potential part of the symmetry energy is very different between the two models, but this has a small effect on the NS EOS.

While sensitive to the high-density values of the symmetry energy, NS observables alone cannot distinguish between the CFG and FFG models. This indicates that the NS EOS, obtained from Bayesian analysis of NS observables is robust and is not sensitive to the exact nuclear model used for the kinetic term of the nuclear symmetry energy.

We thank Bao-An Li and Misak Sargsian for many fruitful discussions. This work was partially supported by the U.S. Department of Energy under grant No. de-sc00006801, the Israel Science Foundation under grant No. DE-FG02-96ER40960, and by the National Science Foundation under grant PHY 1554876.

-
- [1] A. Rios, A. Polls, and W. H. Dickhoff, Phys. Rev. **C89**, 044303 (2014), 1312.7307.
 - [2] S. Gandolfi, J. Carlson, and S. Reddy, Phys. Rev. **C85**,

- 032801 (2012), 1101.1921.
- [3] K. Hebeler, J. M. Lattimer, C. J. Pethick, and A. Schwenk, *Phys. Rev. Lett.* **105**, 161102 (2010), 1007.1746.
- [4] M. Prakash, T. L. Ainsworth, and J. M. Lattimer, *Phys. Rev. Lett.* **61**, 2518 (1988).
- [5] J. M. Lattimer and A. W. Steiner, *Eur. Phys. J.* **A50**, 40 (2014), 1403.1186.
- [6] B.-A. Li and X. Han, *Phys. Lett.* **B727**, 276 (2013), 1304.3368.
- [7] W. G. Lynch, M. B. Tsang, Y. Zhang, P. Danielewicz, M. Famiano, Z. Li, and A. W. Steiner, *Prog. Part. Nucl. Phys.* **62**, 427 (2009), 0901.0412.
- [8] W. Trautmann and H. H. Wolter, *Int. J. Mod. Phys.* **E21**, 1230003 (2012), 1205.2585.
- [9] M. B. Tsang et al., *Phys. Rev.* **C86**, 015803 (2012), 1204.0466.
- [10] B.-A. Li, A. Ramos, G. Verde, and I. Vidana, *Eur. Phys. J.* **A50**, 9 (2014).
- [11] C. J. Horowitz, E. F. Brown, Y. Kim, W. G. Lynch, R. Michaels, A. Ono, J. Piekarewicz, M. B. Tsang, and H. H. Wolter, *J. Phys.* **G41**, 093001 (2014), 1401.5839.
- [12] J. M. Lattimer, *Ann. Rev. Nucl. Part. Sci.* **62**, 485 (2012), 1305.3510.
- [13] M. B. Tsang, Y. Zhang, P. Danielewicz, M. Famiano, Z. Li, W. G. Lynch, and A. W. Steiner, *Phys. Rev. Lett.* **102**, 122701 (2009), [*Int. J. Mod. Phys.*E19,1631(2010)], 0811.3107.
- [14] A. W. Steiner, J. M. Lattimer, and E. F. Brown, *Astrophys. J.* **722**, 33 (2010), 1005.0811.
- [15] R. B. Wiringa, R. Schiavilla, S. C. Pieper, and J. Carlson, *Phys. Rev. C* **89**, 024305 (2014).
- [16] C. Ciofi degli Atti and S. Simula, *Phys. Rev. C* **53**, 1689 (1996), URL <http://link.aps.org/doi/10.1103/PhysRevC.53.1689>.
- [17] A. Carbone, A. Polls, and A. Rios, *Euro. Phys. Lett.* **97**, 22001 (2012).
- [18] I. Vidaña, A. Polls, and C. m. c. Providência, *Phys. Rev. C* **84**, 062801 (2011), URL <http://link.aps.org/doi/10.1103/PhysRevC.84.062801>.
- [19] A. Lovato, O. Benhar, S. Fantoni, A. Yu. Illarionov, and K. E. Schmidt, *Phys. Rev.* **C83**, 054003 (2011), 1011.3784.
- [20] K. Egiyan et al. (CLAS Collaboration), *Phys. Rev. C* **68**, 014313 (2003).
- [21] K. Egiyan et al. (CLAS Collaboration), *Phys. Rev. Lett.* **96**, 082501 (2006).
- [22] N. Fomin et al., *Phys. Rev. Lett.* **108**, 092502 (2012).
- [23] E. Piasezky, M. Sargsian, L. Frankfurt, M. Strikman, and J. W. Watson, *Phys. Rev. Lett.* **97**, 162504 (2006).
- [24] A. Tang et al., *Phys. Rev. Lett.* **90**, 042301 (2003).
- [25] R. Shneur et al., *Phys. Rev. Lett.* **99**, 072501 (2007).
- [26] R. Subedi et al., *Science* **320**, 1476 (2008).
- [27] I. Korover, N. Muangma, O. Hen, et al., *Phys.Rev.Lett.* **113**, 022501 (2014), 1401.6138.
- [28] O. Hen et al. (CLAS Collaboration), *Science* **346**, 614 (2014).
- [29] O. Hen, B.-A. Li, W.-J. Guo, L. B. Weinstein, and E. Piasezky, *Phys. Rev. C* **91**, 025803 (2015), URL <http://link.aps.org/doi/10.1103/PhysRevC.91.025803>.
- [30] O. Hen, L. B. Weinstein, E. Piasezky, G. A. Miller, M. M. Sargsian, and Y. Sagi, *Phys. Rev.* **C92**, 045205 (2015), 1407.8175.
- [31] A. W. Steiner, J. M. Lattimer, and E. F. Brown, *Astrophys. J.* **765**, L5 (2013), 1205.6871.
- [32] B.-J. Cai and B.-A. Li, *Phys. Rev.* **C93**, 014619 (2016), 1509.09290.